Proceedings of the 10th World Congress on Civil, Structural, and Environmental Engineering (CSEE 2025)
Barcelona, Spain - April, 2025
Paper No. 119
DOI: 10.11159/icsect25.119

Challenges in the Anthropocene: Concrete Modified with Pumice Stone Powder from Demolished Block

Bolívar Maza[1], Cristhian Pullaguari[2], Daniela Maza[3]
[1]Universidad Técnica Particular de Loja
San Cayetano Alto, Loja, Ecuador
First. bhmaza@utpl.edu.ec
Second. cfpullaguari@utpl.edu.ec
Third. dsmaza@utpl.edu.ec

Abstract - The increasing demand for Ordinary Portland Cement (OPC) and the high CO_2 emissions generated during its manufacturing process have led to significant efforts to reduce the use of OPC in concrete and decrease CO_2 emissions through pozzolanic materials. Pumice block debris (PBD) from demolition contains products exposed to high temperatures in the past, imparting pozzolanic properties. The chemical composition of PBD was studied, and the aggregate properties were characterized to produce standard concrete (PC) with a strength of 26 MPa, as well as modified concrete (MC). PBD was used as a partial replacement for OPC in varying percentages by weight. The investigative model includes three levels for each substitution variable: PC0%, MC3%, MC6%, MC9%, MC12%, and MC15%. The results were evaluated using inferential statistics. Workability and compressive strength were assessed at 7, 14, and 28 days of curing. The results indicate that increasing the substitution percentage decreases the slump. The compressive strength is highest for MC6%, showing a 5.56% increase compared to standard concrete. The pozzolanic activity index was found to be 77.71%, which is higher than the minimum required value of 75%. It is reported that CO_2 emissions are reduced by 16.62 kg CO_2/m^3 of modified concrete.

***Keywords*:** OPC; Modified concrete; PBD; Emissions; Pozzolanic activity

1. Introduction

The Ordinary Portland Cement (OPC) industry is the third-largest source of air pollution globally, responsible for 8% of global carbon dioxide (CO_2) emissions [1]. OPC production generates nitrogen oxides and volatile organic compounds that can form photochemical ozone in the air, affecting human health and ecosystems [2]. China is the world's largest OPC producer, accounting for 57.1% of global production [3]. In 2020, China's production reached 2400 million tons, leading to severe air pollution problems [4]. In 2019, Ecuador recorded an OPC production of 6 million tons with the highest per capita consumption at 355 kg/person [2].

The production of OPC requires high-temperature combustion during clinker production, resulting in CO_2 emissions and depletion of natural resources [5]. Between 50% and 60% of emissions arise from the decomposition of limestone (Guo et al., 2023). Technical deficiencies, the use of outdated machinery, and poor sustainability management in the OPC concrete production process directly contribute to anthropogenic CO_2 emissions [6].

Currently, the partial replacement of OPC with Supplementary Cementitious Materials (SCM) in concrete has become significant for sustainability [7]. Pozzolanic materials such as fly ash, silica fume, blast furnace slag, rice husk ash, and pumice (PP) have been used to reduce the amount of OPC in concrete [8]. Pozzolans are siliceous and aluminous materials that react with calcium hydroxide [Ca(OH)2] in the presence of water, forming compounds with cementitious properties [9] The use of these materials in concrete production reduces waste disposal in landfills [10]

In this context, the question arises: Is the partial replacement of OPC with pumice block powder from demolition (PR-OPC-PBDFD) sustainable? This study investigates the reduction of OPC consumption in the manufacturing of Modified Concrete (MC). The objective is to find the optimal percentage of PR-OPC-PBDFD by evaluating the properties of MC.

2. Materials

OPC type GU was used, conforming to the specifications of the NTE INEN 2380 (2011) standard, from the Atenas factory in Ecuador. PBD was obtained and ground into a powder with a maximum particle size of 75 µm. The aggregate materials were sourced from the "Junior Acumulada Código 600524" mining area in Chinguilamaca, Province of Loja, and were characterized for the purpose of concrete mix design in accordance with [11]. Figures 1a and 1b show the particle size distribution. For the concrete mix design, the physical properties of the aggregates were evaluated through laboratory tests, with the results presented in Table 1.

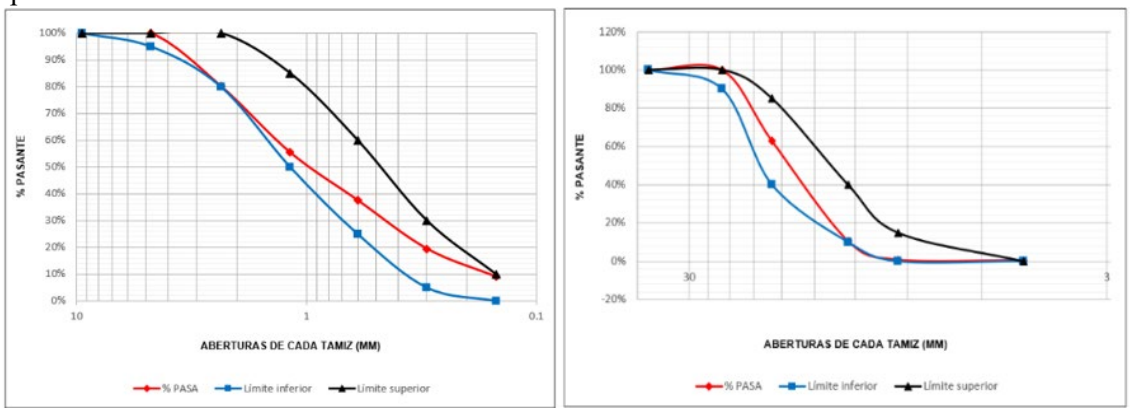

Fig. 1-a - b. Particle size distribution curves for fine and coarse

Table 1. Physical properties of the aggregates.

Parameter	Fine	Coarse	Standard
Compacted unit weight (kg/m^3)	1823.06	1499.79	NTE INEN 858 (2010)
Compacted unit weight (kg/m^3)	1641.51	1376.04	NTE INEN 858 (2010)
Density (SH) (kg/m^3)	2512.50	2664.86	NTE INEN 856 – NTE INEN 857 (2010)
Fineness modulus	2.98	-	NTE INEN 696 (2011)
Nominal maximum size (mm)	-	19	NTE INEN 696 (2011)
Absorption (%)	1.64	0.76	NTE INEN 856 – NTE INEN 857 (2010)
Moisture (%)	3.00	0.10	NTE INEN 862 (2011)

A total of 54 cylindrical concrete specimens were fabricated, including standard specimens and modified concrete specimens with partial substitution of PBD at 3%, 6%, 9%, 12%, and 15% by weight of OPC. The production of 9 specimens for each type of concrete allowed for the determination of compressive strength at 7, 14, and 28 days of curing according to [12]

3 Methodology

PBDFD is obtained through manual crushing, where the material is separated into 3 groups and then subjected to grinding for 2 hours until achieving a maximum particle size of 75 µm (Figure 3) [13]. 5 g of PBDFD were used to conduct X-ray Fluorescence (XRF) testing to study its chemical composition and evaluate its use as a pozzolanic material according to the requirements of [14] standard. The mineral phase of PBDFD is determined through X-ray diffraction (XRD).

Fig. 3. Shows the PBDFD with a particle size of 75 µm.

Mortar Patrón (PM) and Test Mortar (TM) were prepared according to the dosages presented in Table 2, following the guidelines of [15] standard to determine the pozzolanic activity index in contact with OPC.

Table 2. Dosage for Standard Mortar and Test Mortar

Material	Unit	Standard Mortar (PM)	Test Mortar (TM)
OPC	g	450	338
Sand	g	1350	1350
Water	cm^3	225	225
PBD	g	-	112

Note: Adapted from NTE INEN 496 (2015)

For the production of PM and TM, 3 specimens were fabricated for each type of mortar. The specimens are tested at 28 days of curing to determine compressive strength. To evaluate the pozzolanic activity index, the average of the calculated strengths between the two types of mortars is compared using equation 1 [15].

$$I_p = \frac{R}{R_1}\, x\, 100 \tag{1}$$

Given:

- Ip: Pozzolanic activity index with OPC in percentage.
- R:Average compressive strength of the test mortar specimens, in MPa.
- R_1:Average compressive strength of the standard mortar specimens, in MPa.

The design of Standard Concrete (PC) with a strength of 26 MPa was carried out using the [16] method. Table 3 presents the mix proportions. For the production of Modified Concrete (MC), OPC is partially substituted with PBDFD at 3%, 6%, 9%, 12%, and 15% by weight of OPC. The substitution percentages were determined through previous studies. [17] observed that the optimal percentage of partial substitution of OPC with PBDFD is 10%.

Table 3. Mix Proportions for 1 m^3 of Standard Concrete (PC)

Material	Mass (kg)	Ratio	
		Operation	Value
OPC	439.91	439.91/439.91	1.00
Coarse aggregate	900.80	900.80/439.91	2.05
Fine aggregate	768.60	768.60/439.91	1.74
Water	200.46	200.46/439.91	0.46

The Table 4 presents the design used for concrete production, where the codes MC3, MC6, MC9, MC12, and MC15 indicate the substitution percentage.

Table 4. Dosage for Standard Concrete (PC) and Modified Concrete (MC)

Code	Quantity (kg)				
	OPC	Coarse aggregate	Fine aggregate	Water	PBD
PC	8.71	17.78	15.18	4.05	-
MC3	8.45	17.78	15.18	4.05	0.26
MC6	8.19	17.78	15.18	4.05	0.52
MC9	7.93	17.78	15.18	4.05	0.78
MC12	7.66	17.78	15.18	4.05	1.05
MC15	7.40	17.78	15.18	4.05	1.31

Nine cylindrical specimens with a diameter of 100 mm and a height of 200 mm were fabricated for each type of concrete, and compressive strength was determined at 7, 14, and 28 days of curing. The slump was recorded according to [18]. Compressive strength was determined using the Shimadzu Concreto 3000x equipment, applying axial load at a speed of 0.25 ± 0.05 MPa/s [19]. The compressive strength results at 28 days of curing were subjected to normality testing. Based on alternate and null hypotheses, the corresponding statistical test was determined. Statistical analysis was conducted using [20] to ascertain whether the partial substitution of OPC with PBDFD influences the compressive strength of 26 MPa concrete, analyzing the means between each substitution group. To estimate the reduction in CO_2 emissions with the optimal percentage of PBDFD substitution, the amount of CO_2 emitted for the production of 1 m³ of OPC concrete is compared using Equation 2, and emissions generated by the substitution element (PBDFD) during grinding and mechanical sieving stages are compared using Equation 3 [21]. The emission factors are indicated in Table 5.

$$CO_{2-e} = \sum_{i-1}^{n} Q_i \; x \; F_{im} \qquad (2)$$

CO_{2-e}: $kgCO_2$ generated by OPC production.

Q_i: Quantity of material used (kg).

F_{im}: Emission factor of OPC.

Substitution element:

$$CO_{2-e} = \sum P \; x \; t \; x \; F_{im} \qquad (3)$$

CO_{2-e}: $kgCO_2/m^3$ generated by electricity consumption.

P: Power of the equipment (kW).

t: Time of equipment use (h).

F_{im}:Factor for electricity production, 0.29 $kgCO_2$/kWh (Rodríguez et al., 2020).

Table 5. Emission Factors of Materials

Material	FE (kg CO_2/kg)
Cement	0.83
Coarse aggregates	0.0062
Fine aggregates	0.005
Water	0.000196

Note. Adapted from "Effect of incorporation of cane bagasse ash on mechanical properties and carbon dioxide emissions of concrete containing waste glass" (p.5), by Arbeláez Pérez et al., 2019, Bulletin of the Spanish Society of Ceramics and Glass, 62(3).

To obtain PBDFD, grinding is performed in a ball mill with a power of 0.75 kW, and mechanical sieving is performed performed using a Tyler Ro-Tap model Rx-29 with a power of 0.48 kW.

4. Results and Discussion

4.1 X-ray Fluorescence (XRF)

The results of the chemical composition of PP and PBDFD are indicated in Table 6.

Table 6. Chemical Composition of PP and PBDFD Expressed in Percentage

Material (%)	SiO_2	Al_2O_3	Fe_2O_3	CaO	SO_3	K_2O	Ti	Mn
PP	62.50	13.40	0.82	1.55	0.225	2.20	0.16	0.04
PBDFD	63.20	14.00	1.55	9.64	0.97	2.01	0.11	0.05

Note. The presence of OPC in the production of pumice blocks increases the percentage of CaO (9.64%) in PBDFD compared to PP (1.55%).

The chemical analysis of the PP is conducted to compare results with various studies, finding similarity in composition between PP and PBDFD, which shows a higher percentage of CaO due to OPC used in the production of pumice blocks. The histogram in Figure 4 indicates the percentage composition of PBDFD. The chemical requirements of raw or calcined natural pozzolans for use in OPC concrete according to [14] indicate a minimum presence of SiO_2 + Al2O_3 + Fe_2O_3 of 70%, and a maximum presence of SO_3 of 4%. [13] found SiO_2 (74.52%), Al_2O_3 (15.70%), and Fe_2O_3 (3.14%) with the presence of an amorphous chemical structure in PP particles. [22] evaluated PP from Mount Ararat in Turkey and found a presence of SiO_2 + Al_2O_3 + Fe_2O_3 of 84.54%. According to the results found in this research, PBDFD contains 78.75% of SiO_2 + Al_2O_3 + Fe_2O_3, surpassing the minimum percentage according to [14], and SO_3 is present at 0.97%. The chemical composition makes this pozzolanic material a good option to evaluate its suitability as a partial substitute for OPC in concrete. When PBDFD particles react with Portlandite [$Ca(OH)_2$] from OPC, additional calcium silicate hydrate gel forms in the OPC paste, improving the concrete's strength [23].

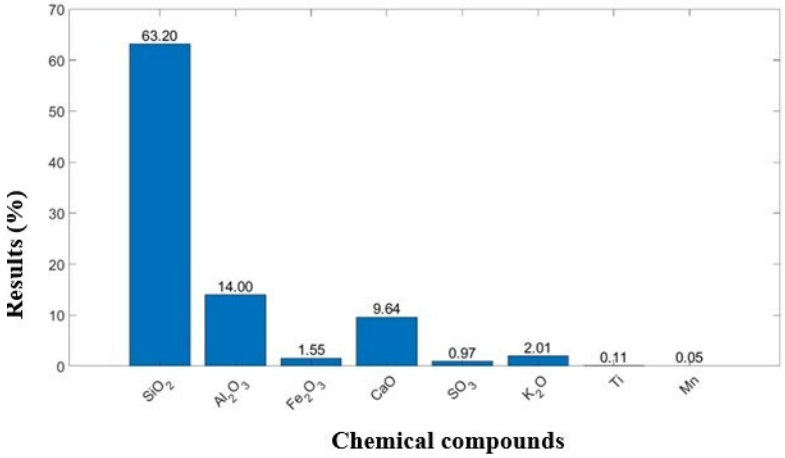

Fig. 4 shows the histogram of the chemical composition of PBDFD

4.2 Pozzolanic Activity Index

Table 7 presents the compressive strength of the standard mortar (PM) and test mortar (TM) at 28 days of curing.

Table 7. Pozzolanic Activity Index

Parameter	Strength (MPa)			Average (MPa)
Standard Mortar	14.69	13.02	13.89	13.87
Test Mortar	10.22	11.84	10.27	10.78
Pozzolanic Activity Index (I_p)				**77.71%**

The pozzolanic activity index of 77.71% exceeds the minimum required percentage of 75% as a physical parameter for natural pozzolans [14]

4.3 XRD Analysis

The mineralogical analysis of PBDFD is illustrated in Figure 5.

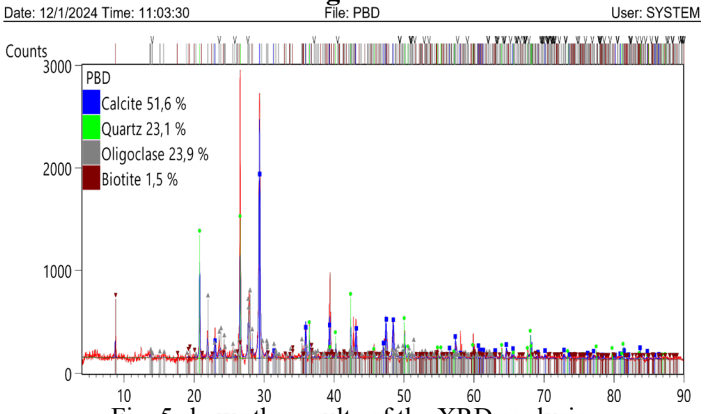

Fig. 5 shows the results of the XRD analysis.

XRD displays the molecular structure; X-ray diffraction is characteristic of each compound. [24] observed the presence of a highly amorphous silica phase in the XRD curve of PP. The amorphous phase is characterized by broad peaks and curves of lower intensity; this phase participates in the chemical reaction with Portlandite from OPC [13]. According to [25], the graph displays the crystalline phase of PP, with the main component being quartz.

4.4 Settlement

Figure 6 depicts the influence of PBDFD substitution percentage on settlement and its variation concerning average compressive strength.

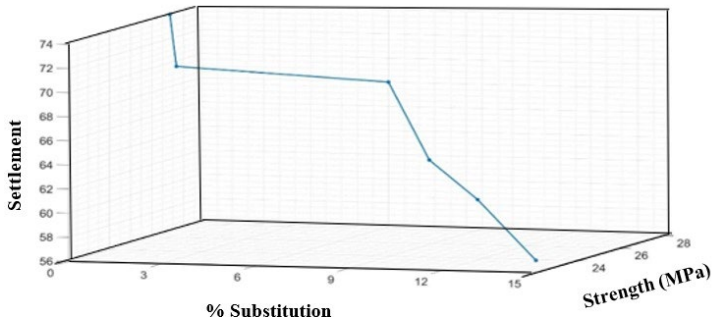

Fig. 6 presents the influence of PBDFD on concrete settlement.

[26] found a decrease in workability of 16% and 28% with 10% and 20% of PP (63 μm), as partial substitution for OPC, similar results to this research. [25] observed that PP at 10%, 20%, and 30% replacement of OPC increased workability by 11.11%, 16.67%, and 27.78%, with a slump of 180 mm in high-strength PC. [23] observed lower workability of concrete with PP at 10%, 15%, 20%, and 25%, with a reduction in the slump diameter of 6.25%, 14.58%, 12.50%, and 27.10%, respectively. [27] observed lower workability of concrete mixes with increasing partial substitution from 10% to 40% of PP (75 μm). In this research, increasing partial substitution of OPC with PBDFD significantly decreases the slump starting from 6% substitution, with a value of 68 mm and a decrease of 6.76% compared to PC. From MC6 onwards, compression decreases significantly. The decrease in slump is due to the porous structure of PBDFD particles, increasing the specific surface area of the material and the requirement for water. Table 9 shows f_c',values.

Table 9. Compressive Strength of PC and MC

Code	7 days	14 days	28 days
	Strength (MPa)	Strength (MPa)	Strength (MPa)
PC	20.36	24.96	26.85
MC3	19.23	20.77	23.16
MC6	17.80	22.71	28.34
MC9	17.96	20.43	25.86
MC12	15.19	17.21	23.73
MC15	15.35	16.50	22.07

4.5 Compressive strength of cylindrical specimens

The compressive strength f_c' is directly proportional to the curing days and decreases as the substitution percentage increases.

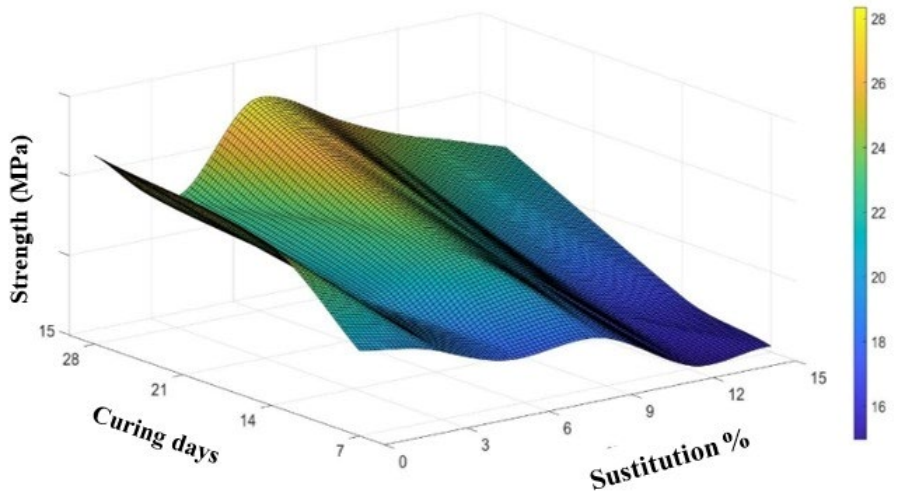

Fig.7 displays values of f_c' curing days, and substitution percentage.

The compressive strength f_c' is directly proportional to the curing days and decreases as the substitution percentage increases. The optimal point for partial substitution of PBDFD for OPC is 6%. [23] evaluated the introduction of PP at 10%, 15%, and 20%, which increased f_c' at 28 days by 14.31%, 9.04%, and 3%, respectively. [28] observed a decrease in f_c' with the introduction of PP at 15% and 20% at 28 days of curing, with reductions of 5.44% and 15.44%, respectively. Saridemir et al. (2016) observed an increase in f_c' at 7, 28, and 56 days with 5% substitution of PP, while the introduction of 10%, 15%, and 20% of PP decreased f_c'. It is ensured that the decrease in strength with increasing PP substitution occurs especially at early ages, and the gap decreases with increasing hydration time [8] .The results of f_c' at 28 days of curing were subjected to a normality test to determine the applicable statistical test according to Table 10. This way, it can be determined if there are significant differences in the average f_c' for each level. The alternative hypothesis (Ha) and null hypothesis (Ho) are stated as follows: Ha: Partial substitution of OPC by PBDFD significantly influences f_c' of 26 MPa concrete. Ho: Partial substitution of OPC by PBDFD does not significantly influencef_c' of 26 MPa concrete. Decision rule: If P < 0.05, Ho is rejected.

Table 10. Normality Test

	Shapiro - Wilk		
Substitution	**Statistic**	**gl**	**P**
PC	0.949	3	0.567
MC3	0.857	3	0.260
MC6	0.953	3	0.582
MC9	0.776	3	0.059
MC12	0.942	3	0.534
MC15	0.933	3	0.501

P>0.05 in all groups, the data present a normal distribution. Apply parametric statistics. The parametric statistical test ANOVA is used to compare the means of the 6 independent groups. Table 11 shows the value of P<0.05, therefore the null hypothesis is rejected and the alternative hypothesis is accepted. The partial substitution of OPC by PBD does influence the compressive strength of 26 MPa concrete; there is a difference between the means.

Table 11. ANOVA Statistical Test

Source of Variation	**Sum of Squares**	**Degrees of Freedom**	**Mean Square**	**F**	**P**	**Critical Value for F**
Between Groups	86.714	5	17.343	9.612	0.001	3.11
Within Groups	21.652	12	1.804			
Total	108.365	17				

4.6 CO_2 Emission Reduction

CO_2 emissions reduction is conducted by comparing the emissions generated for 1 m^3 of OPC concrete. Table 12 presents the results of CO_2 emissions for each type of concrete, and Figure 8 illustrates the reduction in emissions.

Table 12. Emisiones CO_2/m^3 de concreto

TIPO	OPC	Coarse Aggregate	Fine Aggregate	Water	PBD	Emission $kgCO_2/m^3$
PC	439.91	900.80	768.60	200.46	-	374.60
MC3	426.71	900.80	768.60	200.46	13.20	366.29
MC6	413.52	900.80	768.60	200.46	26.39	357.98
MC9	400.32	900.80	768.60	200.46	39.59	349.68
MC12	387.12	900.80	768.60	200.46	52.79	341.37
MC15	373.92	900.80	768.60	200.46	65.99	333.06

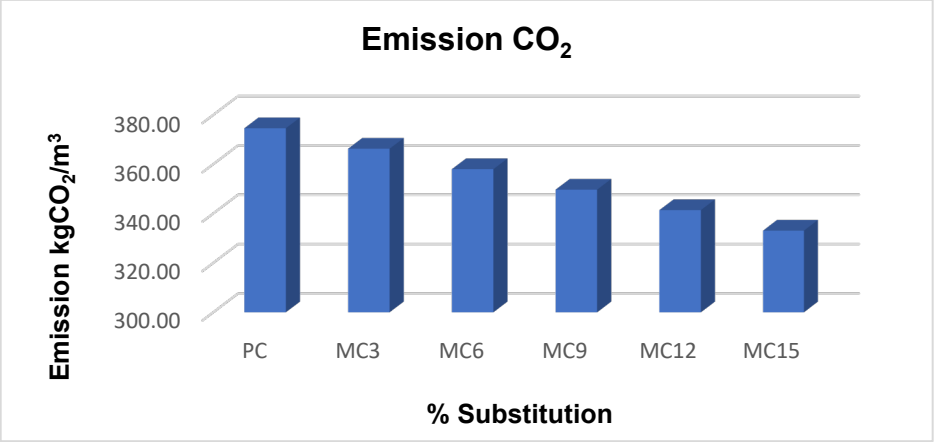

Fig. 8. CO_2 emissions for $1m^3$ of concrete

The manufacturing of PC generates 374.60 kg CO2/m^3, similar to the findings of Arbeláez et al. (2023), who obtained 375 kg CO_2/m^3. The reduction in emissions is significant as the substitution percentage increases by 3%, 6%, 9%, 12%, and 15% of PBD. The CO_2 emissions decrease by 2.22%, 4.44%, 6.65%, 8.87%, and 11.09%, respectively. Considering the production of the optimal percentage MC6, 357.98 kg CO_2/m^3 is generated, reducing 16.62 kg CO_2/m^3. Clearly, this calculation takes into account the grinding and mechanical sieving process of PBD carried out on a small scale, according to sample requirements. The amount of CO_2 released into the atmosphere is proportional to the energy required for the manufacture of OPC (Alqarni, 2022).

5. Conclusions

This research aims to reduce CO_2 emissions in social housing buildings manufactured with MC, evaluating f_c' workability, and the optimal percentage of partial replacement of OPC with PBDFD.

The chemical study revealed that PBDFD has a composition of SiO_2 + Al_2O_3 + Fe_2O_3 at 78.75% and a presence of SO_3 at 0.97%. It was found that the pozzolanic activity index is 77.71%, a value higher than the minimum required of 75%. These properties make PBDFD an ideal material to evaluate its influence on MC. The optimal strength of CM is achieved in MC6 with 28.34 MPa, where the increase is generated by the reaction of PBDFD with Ca (OH)2 from OPC, increasing by 5.56% over PC. The strength decreased with increasing concentration of PBDFD, reaching a minimum value of 22.07 MPa for MC15. Statistical analysis determines that the partial replacement of OPC by PBDFD does influence the compressive strength of 26 MPa concrete.

The addition of PBDFD (75 µm) to concrete produces a decrease in workability of up to 22.97% with 15% replacement, with a minimum slump of 57 mm. MC6 presents a workability of 68 mm due to the porous structure of the particles and their irregular shape, increasing the specific surface area of the material and the requirement for water.

The reduction in CO_2 emissions is significant as the substitution percentage increases. It is concluded that CO_2 emissions are reduced by 16.62 kg CO_2/m^3 of modified concrete.

The results presented make this pozzolanic material a sustainable solution for MC6, with higher compressive strength and reduced CO_2 emission.

References

[1] Tang, L., Ruan, J., Bo, X., Mi, Z., Wang, S., Dong, G. y Davis, S. (2022). Plant-level real-time monitoring data reveal substantial abatement potential of air pollution and CO_2 in China's cement sector. *One Earth,* 5(8), 892-906. https://doi.org/10.1016/j.oneear.2022.07.003

[2] Petroche, D. y Ramírez, A. (2022). The Environmental Profile of Clinker, Cement, and Concrete: A Life Cycle Perspective Study Based on Ecuadorian Data. *Buildings,* 12(3), 1-18. https://doi.org/10.3390/buildings12030311

[3] Adil, W., Rahman, F., Abdullah, G., Tayeh, B. y Zeyad A. (2023). Effective utilization of textile industry waste-derived and heat-treated pumice powder in cement mortar. Construction and Building Materials, 351, 1-3. https://doi.org/10.1016/j.conbuildmat.2022.128966

[4] Ren, M., Ma, T., Fang, C., Liu, X., Guo, C., Zhang, S., Zhou., Z., Zhu, Y., Dai, H. y Huang, C. (2023). Negative emisión technology is key to decarbonizing China's cement industry. *Applied Energy,* 329(120254), 1-16. https://doi.org/10.1016/j.apenergy.2022.120254

[5] Yombi, M. y Chand, J. (2023). Geo-polymer concrete- a concrete for sustainable environment. *IOP Conference Series: Earth and Environmental Science*, 1110(012049), 1-14. https://iopscience.iop.org/article/10.1088/1755-1315/1110/1/012049

[6] Benhelal, E., Shamsaei, E. y Rashid, M. (2020). Challenges against CO_2 abatement strategies in cement industry: A review. *Journal of Environmental Sciences*, 104, 84-101. https://doi.org/10.1016/j.jes.2020.11.020

[7] Wang, Y., Wang, X., Ning, M., He, J., He, J., Lei, Y. y Hou, S. (2023). The collaborative pollutants and carbon dioxide emission reduction and cost of ultra-low pollutant emission retrofit in China's cement kiln. *Journal of Cleaner Production,* 405(136939), 1-9. https://doi.org/10.1016/j.jclepro.2023.136939

[8] Rashad, A. (2021). An Overview of Pumice Stone as a Cementitious Material – the Best Manual for Civil Engineer. *Silicon,* 13, 551-572. https://doi.org/10.1007/s12633-020-00469-3

[9] Tulashie, S., Ebo, P., Ansah, J. y Mensah, D. (2021). Production of Portland pozzolana cement from rice husk ash. *Materialia*, 16, 1-10. https://doi.org/10.1016/j.mtla.2021.101048

[10] Hamada, H., Alattar, A., Yahaya, F., Muthusamy, K. y Tayeh, B. (2021). Mechanical properties of semi-lightweight concrete containing nano-palm oil clinker poder. *Physics and Chemistry of the Earth*, 121(102977), 1-6. https://doi.org/10.1016/j.pce.2021.102977

[11] NTE INEN 872 (2011). *Áridos para hormigón. Requisitos*. Instituto Ecuatoriano de Normalización.

[12] NTE INEN 3124 (2017). *Hormigón. Elaboración y curado de especímenes de ensayo en laboratorio.* Instituto Ecuatoriano de Normalización.

[13] Raheel, M., Khan, H., Iqbal, M., Khan, R., Saberian, M., Li, J. y Ullah, Q. (2023). Experimental investigation of quaternary blended sustainable concrete along with mix design optimization. *Structures*, 54, 499-514. https://doi.org/10.1016/j.istruc.2023.05.033

[14] ASTM C3618 (2019). *Coal Fly Ash and Raw or Calcined Natural Pozzolan for Use in Concrete*. American Society for Testing and Materials.

[15] NTE INEN 496 (2015). *Puzolanas. Determinación del índice de actividad puzolánica. Método del cemento*. Instituto Ecuatoriano de Normalización.

[16] ACI 211.1 (2009). *Standard Practice for Selecting Proportions for Normal, Heavyweight, and Mass Concrete*. American Concrete Institute.

[17] Zeyad, A. Shubaili, M. y Abutaleb, A. (2023). Using volcanic pumice dust to produce high-strength self-curing concrete in hot weather regions. *Case Studies in Construction Materials*, 18(e01927), 1-4. https://doi.org/10.1016/j.cscm.2023.e01927
[18] NTE INEN 1578 (2010). *Hormigón de cemento hidráulico. Determinación del asentamiento.* Instituto Ecuatoriano de Normalización.
[19]NTE INEN 1573 (2010). *Hormigón de cemento hidráulico. Determinación de la resistencia a la compresión de especímenes cilíndricos de hormigón de cemento hidráulico*. Instituto Ecuatoriano de Normalización.
[20] IBM Corp. (2017). *IBM SPSS Statistics for Windows*. Versión 25.0.
[21] Arbeláez, O., Delgado, K. y Castañeda, J. (2023). Efecto de la incorporación de ceniza de bagazo de caña en las propiedades mecánicas y las emisiones de dióxido de carbono del hormigón preparado con residuos de vidrio. *Boletín de la Sociedad Española de Cerámica y Vidrio*, 62, 443-451. https://doi.org/10.1016/j.bsecv.2022.08.001
[22] Karaaslan, C., Yener, E., Bagatur, T. y Polat, R. (2022). Improving the durability of pumice-fly ash based geopolymer concrete with calcium aluminate cement. *Journal of Building Engineering,* 59(105110), 1-5. https://doi.org/10.1016/j.jobe.2022.105110
[23] Özcan, F. y Koç, E. (2018). Influence of ground pumice on compressive strength and air content of both non-air and air entrained concrete in fresh and hardened state. *Construction and Building Materials*, 187, 382-393. https://doi.org/10.1016/j.conbuildmat.2018.07.183
[24]Ghanim, A., Rahman, F., Adil, W., Zeyad, A. y Magbool, H. (2023). Experimental investigation of industrial wastes in concrete: Mechanical and microstructural evaluation of pumice powder and Fly Ash in concrete. *Case Studies in Construction Materials*, 18, 1-16. https://doi.org/10.1016/j.cscm.2023.e01999
[25] Zeyad, A., Tayeh, B. y Yusuf, M. (2019). Strength and transport characteristics of volcanic pumice powder based high strength concrete. *Construction and Building Materials,* 216, 314-324. https://doi.org/10.1016/j.conbuildmat.2019.05.026
[26] Kabay, N., Tufekci, M., Kizilkanat, A. y Oktay, D. (2015). Properties of concrete with pumice powder and fly ash as cement replacement materials. *Construction and Building Materials,* 85, 1-8. http://dx.doi.org/10.1016/j.conbuildmat.2015.03.026
[27] Mboya, H., Njau, K., Mrema, A. y King'ondu, C. (2019). Influence of scoria and pumice on key performance indicators of Portland cement concrete. *Construction and Building Materials*, 197, 444-453. https://doi.org/10.1016/j.conbuildmat.2018.11.228
[28] Madani, H., Naser, M. y Rostami, J. (2018). The synergistic effect of pumice and silica fume on the durability and mechanical characteristics of eco-friendly concrete.*Construction and Building Materials*, 174, 356-368. https://doi.org/10.1016/j.conbuildmat.2018.04.070